Scilight

Transactions on Artificial Intelligence
https://www.sciltp.com/journals/tai

Article

RPGCN-GDA: Regionally Progressive Graph Convolutional Network with Gender-Sensitive Domain Adaptation for EEG Emotion Recognition

Yefei Huang [1], Wei Zhong [2,*], Shuzhan Hu [3,*], Fei Hu [2], Long Ye [2] and Qin Zhang [2]

[1] Key Laboratory of Media Audio & Video (Communication University of China), Ministry of Education, Beijing 100024, China
[2] State Key Laboratory of Media Convergence and Communication, Communication University of China, Beijing 100024, China
[3] School of Data Science and Media Intelligence, Communication University of China, Beijing 100024, China
* Correspondence: wzhong@cuc.edu.cn (W.Z.); hushuzhan@cuc.edu.cn (S.H.)

How To Cite: Huang, Y.; Zhong, W.; Hu, S.; et al. RPGCN-GDA: Regionally Progressive Graph Convolutional Network with Gender-Sensitive Domain Adaptation for EEG Emotion Recognition. *Transactions on Artificial Intelligence* **2025**, *1*(1), 265–281. https://doi.org/10.53941/tai.2025.100018

Received: 30 August 2025
Revised: 9 October 2025
Accepted: 23 October 2025
Published: 5 November 2025

Abstract: Numerous studies have demonstrated that gender-specific emotional patterns are prevalent and can be reflected in electroencephalography (EEG) signals. However, most existing EEG-based emotion recognition models fail to fully account for these gender differences, leading to limited generalization performance. To address this problem, this paper proposes a regionally progressive graph convolutional network with gender-sensitive domain adaptation (RPGCN-GDA). Grounded in prior information of gender differences, the proposed model is expected to flexibly capture gender-specific connectivity patterns across functional brain regions using a progressive graph structure. By fully fusing hierarchical emotional features and adaptively adjusting distributional differences between genders, our model performs remarkable generalization capabilities in both cross-subject and cross-gender emotion recognition tasks. The experiment results on public datasets demonstrate that the model not only excels in subject-dependent and subject-independent tasks but also shows significant advantages in handling gender-specific emotional responses, offering a promising new direction for developing higher gender-sensitive emotion recognition systems.

Keywords: EEG emotion recognition; gender differences; graph convolutional network; domain adaptation

1. Introduction

Emotions, as an expression of internal human psychological responses, are driven by external stimuli and internal cognition. The field of emotion recognition is full of challenges and opportunities, whose advances continue to drive the development of human psychology and human-computer interaction (HCI) applications [1,2]. With the advancement of emerging technologies such as deep learning, emotion recognition based on visual content has achieved significant progress [3]. In recent years, the EEG-based emotion recognition technology has become a research hotspot at the intersection of the fields of neuroscience and computer science[4]. By directly capturing the brain's electrical activity, EEG provides an objective and high temporal resolution representation of neural processes, enabling more accurate and reliable emotion decoding compared to other modalities such as facial expressions or speech.

Traditional machine learning methods, such as SVM [5], have limitations in dealing with the complexity and non-linear features of EEG signals. To overcome these challenges, the deep learning approaches have gained significant attention for their ability to capture intricate patterns in EEG signals. Concretely, the convolutional neural networks (CNNs) excel in encoding spatial features from EEG signals by leveraging their electrode channel structure [6,7], while the recurrent neural networks (RNNs) are adept at modeling the temporal dynamics of sequential EEG signals and tracking emotion changes over time [8,9]. More recently, the graph convolutional networks (GCNs) have

emerged as a powerful tool in EEG emotion recognition due to their ability to effectively capture spatial dependencies between electrodes [10–13]. The connectivity patterns and interactions of the brain regions characterized by these dependencies are directly related to specific emotional activities [14]. Furthermore, in order to better construct the different spatial features exhibited by EEG signals from different brain regions and electrode channels, more and more studies [6,8,9,13] modeled the spatial features progressively from local regions to global connectivity, thereby achieving more comprehensive and interpretable emotion representations.

While in the field of emotion recognition, it is important to realize that the individual differences are particularly pronounced in emotional responses, especially with respect to gender [15]. Established psychological and neuroscience studies have demonstrated significant gender differences in emotional experience, expression and response, which are evident not only in behavioral and psychological aspects but also in physiological reactions, including distinct patterns of brain region activation during emotional processing [16–18]. Despite these insights, few EEG-based emotion recognition models have incorporated gender differences into their design, limiting their ability to adapt to gender-specific variations in emotional responses. Therefore, more gender-sensitive emotion recognition models have yet to be developed for the advance of personalized HCI systems.

Based on the above issues, we propose a regionally progressive graph convolutional network with gender-sensitive domain adaptation (RPGCN-GDA). This model is specifically designed to tackle the challenges posed by gender-specific variations in EEG signals with two core innovations. On one hand, the proposed RPGCN-GDA employs a hierarchical and progressive graph learning structure that models the complex dependencies across electrode channels and brain regions. By integrating prior knowledge of fluctuations in gender differences from differential entropy features, we incorporate gender-specific functional connectivity weights to dynamically adjust the graph topology, better reflecting gender-influenced neural mechanisms. On the other hand, we introduce a gender-sensitive domain adaptation module at the emotion decoding stage, which leverages implicit gender labels to align the distributional differences of EEG features between males and females. This strategy enhances the cross-gender generalization of the model, addressing the inherent domain shift in the cross-gender emotion recognition tasks.

Our main contributions can be summarized as follows:

- We propose a regionally progressive graph convolutional network with gender-specific functional connectivity. It effectively integrates local and global brain region dependencies and considers gender differences from differential entropy features of male and female subjects.
- We introduce the gender-sensitive domain adaptation in our design, which optimizes the transfer learning capability of the model by adjusting the distributional differences between genders.
- We conduct comprehensive experiments on the SEED and SEED-IV datasets. The results demonstrate that the proposed RPGCN-GDA can achieve superior performance in various settings, especially in dealing with gender differences. It proves a new benchmark for gender-sensitive EEG emotion recognition models.

2. Related Works

2.1. Spatial-Temporal EEG Emotion Recognition

EEG signals are a collection of sequences containing both temporal and spatial information, which is reflected in the electrode distribution associated with the activation of different brain regions. Based on the spatial-temporal properties, the researchers have designed diverse and effective emotion recognition models with deep neural networks, such as CNNs and RNNs. Ding et al. [6] proposed a multi-scale CNN named TSception to capture the temporal dynamics and spatial asymmetry of EEG signals. Li et al. [8] designed a bi-hemisphere disparity model (Bi-HDM) based on RNN that takes into account the function of hemispheric regions. Li et al. [9] refined the brain region function and used bidirectional long and short-term memory (Bi-LSTM) to learn spatial features hierarchically from local to global brain regions. Tao et al. [7] combined respective advantages of CNN and RNN to explore spatial and temporal information in EEG. However, these methods are difficult to take into account the functional connectivity between electrode channels and brain regions, and lack sufficient neurological supports for the interpretable modeling of spatial features.

2.2. Graph Neural Networks for EEG

The functional and anatomical structure of the brain can be viewed as a complex network with functional connections between different brain regions. This natural topological structure is particularly suitable for representation using graphs. Generally speaking, a graph constructed from EEG is an undirected graph $\mathcal{G} = (\mathcal{V}, \mathcal{E})$, where $\mathcal{V}$ is the set of channel nodes, and $\mathcal{E}$ is the set of edges reflecting the connectivity of channels, which can also be

described as an adjacency matrix. The GCNs precisely capture the correlation and synchronization cross channels to encode emotions by passing messages between the graph nodes. In related researches, Song et al. [10] designed a dynamical GCN to model the multi-channel EEG features through the learnable dynamic graphs. Zhong et al. [11] introduced neuroscience-inspired priors into EEG graph construction and used the regularization techniques such as adversarial training to reduce individual distributional differences. Zhou et al. [12] integrated coarse-to-fine emotion classification and brain functional connectivity with a Progressive-GCN, uncovering the link between emotions and EEG features. Jin et al. [13] proposed the pyramidal structure for affective graph learning, constructing the hierarchial graph features at multiple scales from EEG channels to brain regions.

2.3. Gender Differences in EEG Emotion Recognition

Considering the fact that gender is an influential factor in emotional processing, some researchers attempted to investigate the neural patterns reflecting gender differences with EEG. Zhu et al. [19] tentatively identified the existence of gender differences in their study of the individual emotional change within EEG. Yan et al. [20] explored key brain regions associated with specific emotions in both genders through LSTM networks. In their further research [21], they designed a bimodal deep autoencoder to integrate EEG and eye movement data and observed gender differences in multimodal emotion recognition. Against this backdrop, Li et al. [22] further explored gender differences in critical frequency bands and channels of EEG signals by using a single-modality attentive simple graph convolutional network (ASGC). Later, Peng et al. [23] expanded the samples of subjects across more datasets and applied the ASGC to prove that gender is a crucial factor affecting the performance of EEG-based emotion recognition models. The above studies have demonstrated the existence of gender differences in EEG emotion recognition and identified it as an influential factor which cannot be ignored. While few research works have incorporated this factor into the model design and provide specialized affective computing solutions tailored to address gender differences.

3. Method

To illustrate the proposed method more clearly, we show the framework of RPGCN-GDA in Figure 1. It mainly consists of two functional blocks: emotion encoder and emotion decoder. At the emotion encoding stage, the hierarchical graph encoder dynamically models the differential entropy (DE) features extracted from the subjects in physical space, and mines them on functional connectivity with brain regions in a regionally progressive manner. In particular, we calculate the absolute differences in DE features between the two sex domains as prior gender knowledge, helping to construct a gender-specific connectivity matrix to enhance the gender sensitivity of model. Then the multilevel fused-graph encoder globally aggregates emotion features across layers and integrates emotional information at different scales with an attention block. In the emotion decoding process, the model decodes the fused emotion features by multilayer perceptron and simultaneously reduces the effect of gender-differentiated distributions through the domain adaptation module, thus completing the final emotion recognition task.

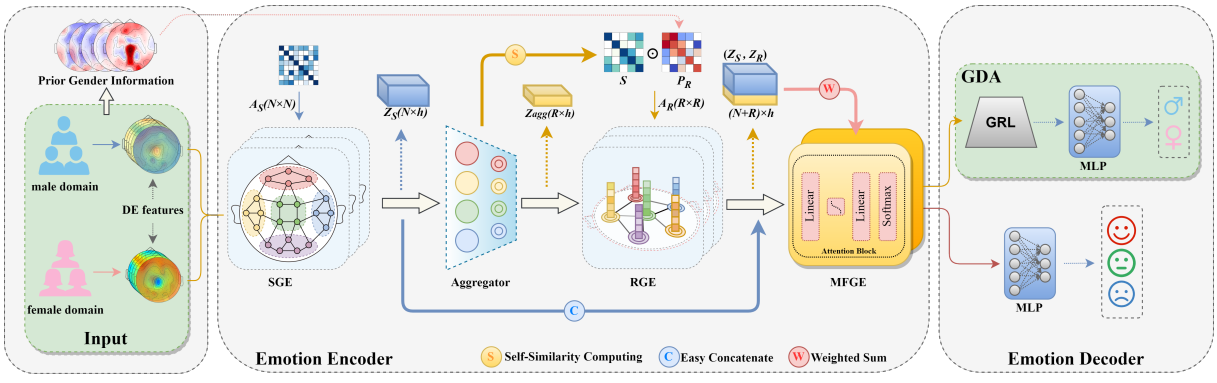

Figure 1. Overall framework of RPGCN-GDA for EEG-based emotion recognition. SGE and RGE denote Spatial Graph Encoder and Regional Graph Encoder, and they are cascaded through an aggregator. MFGE denotes Multilevel Fused-Graph Encoder. GDA denotes Gender-Sensitive Domain Adaptation.

3.1. Hierarchical Graph Encoder

The hierarchical graph encoder consists of cascading graph learning blocks. It is differentiated into graph encoders with different functions based on different adjacency matrix. The graph learning block mainly utilises simplified graph convolution (SGC) [24] to dynamically learn graph representations. The SGC reduces model

complexity while maintaining the modelling capability of GCNs.

3.1.1. Spatial Graph Encoder

The spatial graph encoder (SGE) is designed to initially and efficiently extract cross-channel spatial-temporal features from the input DE features, which have been proven by most studies to have excellent emotional representation capabilities [25]. Let $\mathbf{X} \in \mathbb{R}^{N \times f}$ be the input matrix of DE features, where N is the number of electrode channels and f is number of frequency bands. Then we define the output of the SGE as $\mathbf{Z}_{\mathcal{S}}$ and the processing operation can be represented as:

$$\mathbf{Z}_{\mathcal{S}} = \Phi_{\text{ReLU}} \left(\text{BN} \left(\hat{\mathbf{A}}_{\mathcal{S}}^{K} \mathbf{X} \mathbf{W}_{\mathcal{S}} \right) \right), \tag{1}$$

where $\hat{\mathbf{A}}_{\mathcal{S}} = \mathbf{D}^{-1/2} \mathbf{A}_{\mathcal{S}} \mathbf{D}^{-1/2}$ is a symmetrically normalized adjacency matrix representing spatial information, $\mathbf{D}$ is the degree matrix, $\mathbf{W}_{\mathcal{S}} = \mathbf{W}_{\mathcal{S}}^{(1)} \mathbf{W}_{\mathcal{S}}^{(2)} ... \mathbf{W}_{\mathcal{S}}^{(K)}$ is the re-parameterized and learnable weight matrix, Φ_{ReLU} is the activation function. In the graph learning block, K is the step of feature propagation and set to 2 to implement a two-order convolution, such that the node feature vector is related to its direct and second-order neighbors. It is worth mentioning that both matrix sparsity and low-order K value are set to effectively prevent over-smoothing of the graph convolution layer [13]. In the graph encoder, we use batch normalization (BN) and ReLU activation layers to stabilize the training process and increase the nonlinear expressiveness of the model. The total encoding process of a complete graph encoder can be described as Figure 2.

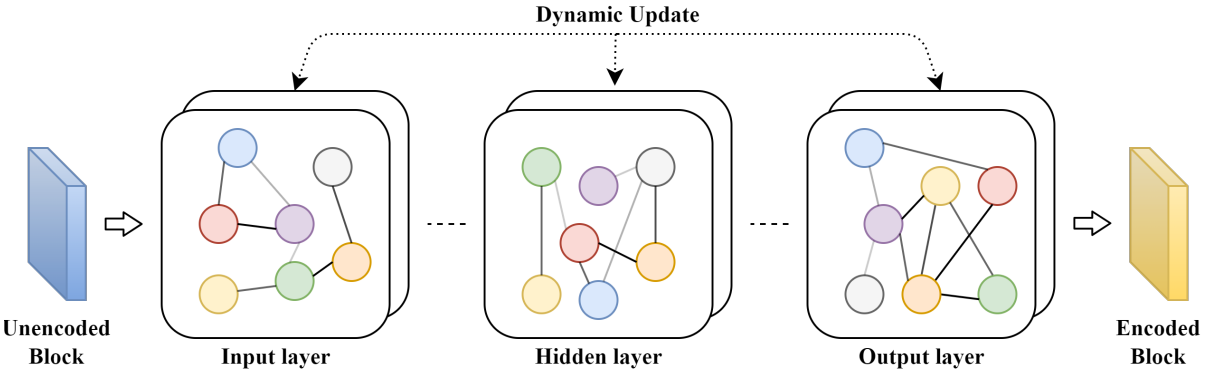

Figure 2. The encoding process of the graph encoder.

Drawing on the experience of RGNN [11] and PGCN [13], we construct $\mathbf{A}_{\mathcal{S}} \in \mathbb{R}^{N \times N}$ as a sparse adjacency matrix to describe the connection of channels based on the relative spatial positions of EEG electrodes. The elements a_{ij} contained are determined by the 3D Euclidean distance d_{ij} between electrodes i and j:

$$a_{ij} = \begin{cases} 1 & \text{if } d_{ij} \leq d_{\text{thresh}} \\ \frac{\delta}{d_{ij}^2} & \text{if } d_{\text{thresh}} < d_{ij} \leq d_{\max} \\ 0.1 & \text{if } d_{ij} > d_{\max} \end{cases}, \tag{2}$$

where δ is the sparsity factor and set to 5 by referring to the work of RGNN [11], d_{thresh} and $d_{\max}$ are the distance thresholds to control the sparsity of the graph connections. The design allows the graph learning block to focus on strong connections to neighboring electrodes and reserve global information.

Inspired by the fact that the connection strength and pattern of different brain regions dynamically change with different cases, the spatial-temporal adjacency matrix $\hat{\mathbf{A}}_{\mathcal{S}}$ is adaptively updated with the parameter changes during the model training. In this way, the model is able to dynamically adjust the EEG channel connections for adaptive graph-based data driven.

3.1.2. Regional Graph Encoder

Emotional networks in the brain usually consist of multiple interconnected regions and different regions of the cerebral cortex show a certain degree of functional differentiation during emotional processing [14]. According to neurological findings, Figure 3 shows the classification of brain regions with different basic cognitive functions [26]. It has been analyzed that [20], the functional connectivity patterns in different regions of the brain show significant gender differences during emotional processing and regulation. Therefore, it is necessary to consider the global

functional connectivity of the brain regions with gender specificity in emotions when constructing the EEG-based emotion recognition models.

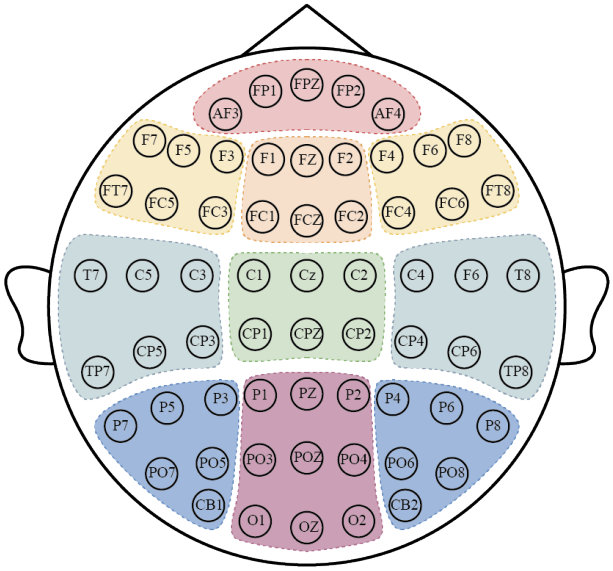

Figure 3. 62-channel EEG electrode distribution with 10-region layouts.

The regional graph encoder (RGE) is designed to analyze their complex dependencies of aggregated information within different functional brain regions. It introduces prior gender information while further extracting key emotional information of the functional connectivity of brain regions. The aggregator serves as a bridge between SGE and RGE and embodies the idea of regionally progressive feature aggregation. Firstly, we divide the 62 electrodes into 10 electrode clusters according to the regional function classification of the brain in Figure 3. Assuming that the r-th region contains an electrode set of $\mathcal{C}_r$, the aggregated features $\mathbf{z}_r$ can be expressed as the average of all the electrode features within this region:

$$\mathbf{z}_r = \frac{1}{|\mathcal{C}_r|} \sum_{i \in \mathcal{C}_r} \mathbf{z}_{\mathcal{S}}^i \in \mathbb{R}^{1 \times h}, \quad r \in [1, 10], \tag{3}$$

where $\mathbf{z}_{\mathcal{S}}^i$ is the spatial-temporal feature of the i-th electrode in the r-th region ($i \in [1, |\mathcal{C}_r|]$) output from SGE and h is the mapping dimension of the feature. In this way, we compress the features of 62 electrodes into 10 functional regions and get an aggregated feature matrix $\mathbf{Z}_{\text{agg}} = \{\mathbf{z}_r\}_{r=1}^R$, where R is the number of classified brain regions. The construction of the adjacency matrix based on self-similarity [27] of node features is suitable for constructing dynamic graph and capturing global information. Inspired by this, we then compute the self-similarity matrix $\mathbf{S}$ in which each element s_{ij} represents the feature similarity between the i-th and j-th regions:

$$\mathbf{S} = \mathbf{Z}_{\text{agg}} \mathbf{Z}_{\text{agg}}{}^{\top} \in \mathbb{R}^{R \times R}. \tag{4}$$

During the back propagation process, the self-similarity connection weight $\mathbf{S}$ is dynamically calculated to better capture the variable dependence between the brain regions with the adaptive graph.

In order to enhance the sensitivity of the model to gender differences, we consider introducing the gender-specific functional connectivity weights $\mathbf{P}_{\mathcal{R}}$ into RGE, which is essentially a mathematical representation of how brain region connections differ between males and females during emotional processing. And it will be described in detail in Section 3.2. The regionally progressive adjacency matrix $\mathbf{A}_{\mathcal{R}}$ of RGE is computed as follows:

$$\mathbf{A}_{\mathcal{R}} = \Phi_{\text{ReLU}}(\mathbf{S} \odot \mathbf{P}_{\mathcal{R}}). \tag{5}$$

Then we can obtain the output of RGE denoted as $\mathbf{Z}_{\mathcal{R}}$ by regionally encoding through convolutional operation of the aggregated emotion feature $\mathbf{Z}_{\text{agg}}$ as shown in Figure 2:

$$\mathbf{Z}_{\mathcal{R}} = \Phi_{\text{ReLU}} \left(\text{BN} \left(\hat{\mathbf{A}}_{\mathcal{R}}^K \mathbf{Z}_{\text{agg}} \mathbf{W}_{\mathcal{R}} \right) \right), \tag{6}$$

where $\mathbf{W}_{\mathcal{R}} = \mathbf{W}_{\mathcal{R}}^{(1)} \mathbf{W}_{\mathcal{R}}^{(2)} ... \mathbf{W}_{\mathcal{R}}^{(K)}$ is the K-weighted learnable parameter matrix similar to (1).

3.2. Connectivity Weights from Prior Gender Information

In this section, we explore the integration of prior gender information derived from DE features of subjects and construct a gender-specific connectivity matrix applied in RGE to enhance the sensitivity of the model.

In order to analyze the gender differences of brain activation, we calculate the average normalized DE features for subjects with the same gender in multiple emotional states. Then the regional fluctuations in gender differences are expressed by DE feature difference and visualized in the brain topography as shown in Figure 4. Obviously, the significant differences in neural activity between genders are reflected in multiple brain regions and frequency bands (i.e., δ, θ, α, β, γ). Concretely, the males present stronger activation in the parietal and occipital regions. And in other regions the activation level in females increases with increasing frequency bands. These findings are consistent with the previous studies [20,22,23].

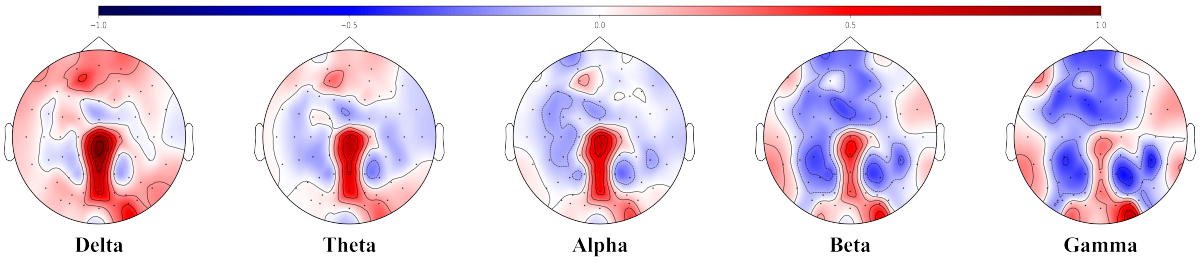

Figure 4. The brain topography differences between males and females with the average normalized DE features on the SEED-IV dataset.

To systematically incorporate this prior gender information into the model, we leverage the DE differences to construct $\mathbf{P}_{\mathcal{R}} \in \mathbb{R}^{R\times R}$ as gender-specific functional connectivity weights. Specifically, we further compute the DE difference through the manner of regionally average aggregation. Assuming that each brain region has the corresponding δ_i of DE differences to indicate its degree of regional differentiation, then the gender-specific functional connectivity weight between two regions can be measured using the Pearson correlation coefficient:

$$\mathbf{P}_{\mathcal{R}} = \begin{bmatrix} \boldsymbol{p}_{1,1} & \cdots & \boldsymbol{p}_{1,R} \\ \vdots & \ddots & \vdots \\ \boldsymbol{p}_{R,1} & \cdots & \boldsymbol{p}_{R,R} \end{bmatrix}, \tag{7}$$

$$\boldsymbol{p}_{i,j} = \frac{\operatorname{cov}(\delta_i, \delta_j)}{\sigma(\delta_i)\,\sigma(\delta_j)}, \quad i,j \in [1,R], \tag{8}$$

where $\operatorname{cov}(\cdot)$ denotes the covariance operation and $\sigma(\cdot)$ denotes the standard deviation operation. The correlation index $\boldsymbol{p}_{i,j}$ is within the range $[-1,1]$. By integrating $\mathbf{P}_{\mathcal{R}}$ into the construction of $\mathbf{A}_{\mathcal{R}}$ as shown in (5), the RGE is expected to dynamically assign gender-related functional weights to emotional features, thus better capturing gender-specific neural activity patterns.

3.3. Multilevel Fused-Graph Encoder

The multilevel fused-graph encoder (MFGE) is a key module in our model that balances feature fusion with final emotion encoding. It effectively exploits key emotional information from SGE and RGE and allocates spatial attention resources for better encoding emotional patterns. Specifically, the input of MFGE is the concatenation of the embedded features $\mathbf{Z}_{\mathcal{S}}$ and $\mathbf{Z}_{\mathcal{R}}$. And the importance of different embeddings is then weighted by the attentional mechanism.

Taking one embedding $\mathbf{z}_s^i \in \mathbb{R}^{1\times h}$ ($\mathbf{Z}_{\mathcal{S}} = \{\mathbf{z}_s^i\}_{i=1}^N \in \mathbb{R}^{N\times h}$) as an example, where N denotes the number of nodes and h denotes the feature dimension, we perform a nonlinear mapping on $\mathbf{z}_s^i$ and the spatial self-attention score assigned to the i-th node can be expressed as:

$$\omega_s^i = \mathbf{q}^\top \cdot \tanh(\mathbf{W}\cdot(\mathbf{z}_s^i)^\top + \mathbf{b}), \quad i \in [1,N], \tag{9}$$

where $\mathbf{W} \in \mathbb{R}^{h'\times h}$ is the shared weight matrix and $\mathbf{b}$ is the bias vector. Meanwhile, the attention value of each node is computed using an equally shared linear dimensionality reduction vector $\mathbf{q} \in \mathbb{R}^{h'\times 1}$. Similarly, the attention value ω_r^i obtained from the regional embeddings $\mathbf{Z}_{\mathcal{R}}$ can be calculated in the same way:

$$\omega_r^i = \mathbf{q}^\top \cdot \tanh(\mathbf{W}\cdot(\mathbf{z}_r^i)^\top + \mathbf{b}), \quad i \in [1,R]. \tag{10}$$

Finally, we can compute the self-attention weights of channel-nodes and region-nodes as $\boldsymbol{\beta_s}$ and $\boldsymbol{\beta_r}$ from embedded features of $\mathbf{Z}_{\mathcal{S}}$ and $\mathbf{Z}_{\mathcal{R}}$ respectively,

$$\beta_s^i = \text{softmax}\left(\omega_s^i\right) = \frac{\exp\left(\omega_s^i\right)}{\exp\left(\omega_s^i\right) + \exp\left(\omega_r^i\right)}, \tag{11}$$

$$\beta_r^i = \text{softmax}\left(\omega_r^i\right) = \frac{\exp\left(\omega_r^i\right)}{\exp\left(\omega_s^i\right) + \exp\left(\omega_r^i\right)}. \tag{12}$$

The fused embedding feature through the self-attention mechanism is obtained as $\mathbf{Z}_{\text{out}} = \boldsymbol{\beta_s}^\top \mathbf{Z}_{\mathcal{S}} + \boldsymbol{\beta_r}^\top \mathbf{Z}_{\mathcal{R}}$, which integrates affective information from spatial channels and brain regions.

3.4. Emotion Decoder with Gender-Sensitive Domain Adaptation

In the following process, the multilevel fused graph embedding $\mathbf{Z}_{\text{out}}$ is further processed through BN, ReLU activation and a dropout layer. And the model completes the process of emotion decoding through a two-layer fully connected network.

In addition, inspired by the work of Gu et al. [28], we introduce a branch of domain adaptation based on gender labeling that focuses on dealing with the impact of gender differences on emotion recognition. In order to address the challenge of individual differences in the distribution of EEG features, the GDA module is designed to divide the subjects into different domains according to implicit gender labels. Afterwards, the domain adversarial mechanism is employed to reduce the differences in feature distributions between different gender domains, thus enhancing the robustness of the model.

In concrete terms, we introduce a domain classifier D to estimate the probability of the gender domain to which the encoding feature belongs. The domain classifier D is structured as a fully connected linear layer with optimization parameters θ_D, and the outputs are dichotomous labels corresponding to male and female, respectively. Then we optimize the domain classifier by minimizing the domain classification loss $\mathcal{L}_D$:

$$\begin{aligned}\mathcal{L}_D = -\frac{1}{N}\sum_{i=1}^{N}[y_i \log(p(D(x_i;\theta_D))) \\ + (1-y_i)\log(1-p(D(x_i;\theta_D)))],\end{aligned} \tag{13}$$

where x_i is the i-th sample and y_i is the gender label. Following the previous work [28–30], a gradient reversal layer (GRL) is employed to reverse the gradient of the domain classifier D. The final loss is obtained as the weighted sum of emotion classification loss $\mathcal{L}_E$ and domain classification loss $\mathcal{L}_D$:

$$Loss = \mathcal{L}_E + \lambda \mathcal{L}_D, \tag{14}$$

where $\lambda = \left(\frac{2}{1+e^{-10t}}\right) - 1$ ($t \in [0,1]$) is a weight hyperparameter to balance the effects of different loss terms. In the decoding stage, λ can be dynamically adjusted according to the training progress t. This design directly follows the classic scheduling strategy proposed by Ganin et al. [31] and has been further validated its superiority in balancing feature learning and domain alignment [32]. Similar designs have also been widely adopted in EEG signal processing [28,30,33]. This scheduling strategy effectively prevents domain adaptation from being misled by inadequately optimized feature learning at the early stage of training procedure, thereby ensuring training stability.

It should be noted that within the RPGCN-GDA model, the branch of GDA employs a domain adversarial mechanism to assist the main branch in strengthening the model's generalization performance in cross-individual at the emotion decoding stage. The function of the GDA is specifically designed for the scenario of cross-subject or cross-gender transfer learning-based emotion recognition. Conversely, in the subject-dependent emotion recognition tasks, the model operates as RPGCN by removing the GDA module. In this mode, the main decoding branch functions independently, utilizing a fully connected layer with the softmax function to decode the emotion state of a single subject.

4. Experiments

In the experimental design, we conduct our experiments on the SEED and SEED-IV datasets. In order to fully evaluate the performance of the proposed model, we perform the subject-dependent and subject-independent experiments and make comparison with existing studies.

In the subject-dependent experiment, the model is trained and tested using data from a single subject only.

Each subject in the SEED dataset [34] went through 15 trials of movie clips, and we use the data from the first 9 trials as the training set and that from the remaining 6 trials as the testing set. For the SEED-IV [35], there are 24 trials per subject, where the data from the first 16 trials is used for training and the last 8 trials for testing. In the subject-independent experiments, the model is evaluated by leave-one-subject-out (LOSO) cross-validation. Specifically, for the 15 subjects in the SEED and SEED-IV datasets, each subject is sequentially rotated to serve as the testing set, with the remaining 14 subjects as the training set, in which case this process was repeated 15 times. We calculate the average accuracy/standard deviation (ACC/STD) across all subjects for three sessions of each dataset as the performance evaluation metrics.

To assess the performance in gender sensitivity and cross-gender emotion recognition, we also design a set of gender-specific assessment strategies and validate the effectiveness of the proposed model through comparisons with other methods and ablation experiments. As shown in Figure 5, we follow the work [21–23] in developing same-gender and cross-gender strategies based on cross-subject scheme. The results on these two strategies will be independent of those on subject-independent experiments as mixed-gender strategy. The same-gender strategy requires that both the training and testing data comes from the same gender group, whereas the cross-gender strategy is the reverse. Specifically, the same-gender strategy is used to train the same-gender model by LOSO in same gender group, including the training of the M-M model and F-F model. While the cross-gender strategy performs LOSO cross group, i.e., the cross-gender model for each subject in the same group is trained by opposite-sex subjects in the other group, including the training of the F-M model and M-F model. The performance of all models is evaluated using the average metrics of a single group as the final reference. Ultimately, we compare the predictive accuracy of models trained with same-gender and cross-gender strategies in order to assess the universality and specificity of neural patterns cross genders. Moreover, we further test the robustness of the proposed model under imbalanced gender data to reflect real-world deployment.

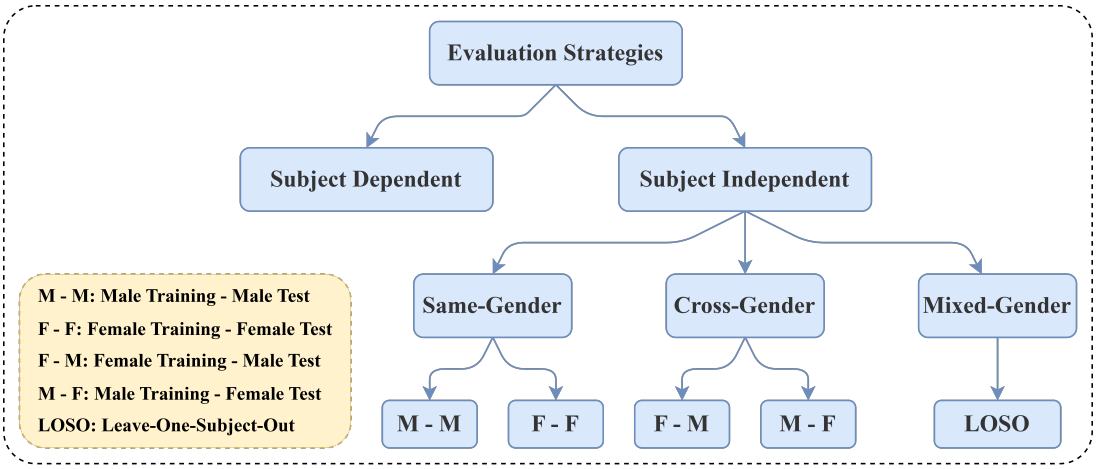

Figure 5. Evaluation strategies for subject-dependent and subject-independent experiments.

The model is trained using the adaptive optimizer Adam. For more details on training process, all hidden layers of the model are set to 30 with a dropout coefficient of 0.5. The number of epochs is set to 300 for the training process. The learning rates are set to 1e-4 and 5e-5, and the batch sizes are set to 64 and 32 in the subject-dependent and subject-independent experiments, respectively. All models in the experiments are deployed and trained under a unified hardware and software environment. The hardware configuration consists of an NVIDIA GeForce RTX 2080 Ti GPU (21.7 GB VRAM) and an Intel(R) Xeon(R) CPU E5-2640 v4 (252 GB RAM). The software environment includes PyTorch 2.1.1, CUDA 11.8, and Python 3.10.0. The corresponding RPGCN-GDA model contains 5.14 million parameters, achieves an inference time of 6.58 ms per EEG sample, utilizes 13.25 MB of GPU memory, and requires 4.46 million FLOPs.

4.1. Comparisons with Competing Methods

In this section, we evaluate the performance of our model on the SEED and SEED-IV datasets with the subject-dependent and subject-independent experiments separately. The comparison results with other representative methods are shown in Table 1.

It can be seen from Table 1 that the proposed RPGCN-GDA exhibits superior classification accuracies in both subject-dependent and subject-independent experiments. It achieves the accuracies of 96.68% and 87.55% on the SEED dataset as well as 83.05% and 73.67% on the SEED-IV dataset, respectively. Compared to the methods

such as SVM [5], MS-MDA [30], Bi-HDM [8] and R2G-STNN [9], the GNN-based methods demonstrate the advantages in capturing the intricate spatial dependencies of EEG signals. When compared to GNN-based models like DGCNN [10], RGNN [11] and Progressive-GCN [12], our model surpasses these single-level graph learning structures, proving that the regionally hierarchical encoding can be a more effective and explicable graph learning approach for EEG-based emotion recognition tasks. Furthermore, compared to the latest Pyramidal-GCN [13] that similarly employs a regionally hierarchical graph learning structure, our model remains competitive.

In particular, the proposed RPGCN-GDA shows the comparable accuracy to Pyramidal-GCN [13] on SEED-IV (73.67% vs. 73.69%) in the subject-independent scenario, while achieving a lower standard deviation (4.55% vs. 7.16%) and showing better robustness. Similar trends are also observed on the SEED dataset for the subject-dependent experiment. Specially, the improvement of 3% compared to Pyramidal-GCN [13] in cross-subject performance on the SEED dataset further demonstrates the strong generalization capability of our RPGCN-GDA in adapting to individual differences in EEG signals. It can be attributed to the incorporation of regionally progressive graph encoding and gender-sensitive domain adaptation decoding, which enables our model to address domain shifts caused by individual differences.

Furthermore, to optimize spatial feature extraction for EEG-based emotion recognition by leveraging region-specific brain activation mechanisms during distinct cognitive processes [14], we employ three brain region partitioning methods (7-region, 10-region and 17-region) for electrode clustering, following the methodology in [36]. The neuroscientific research indicates that the brain functional networks exhibit modular organization, and the default mode network (DMN) plays a critical role in emotional processing with significant gender differences in its functional connectivity [37]. As shown in Figure 6, the 10-region brain partition outperforms 7/17-region partitions on both of the SEED and SEED-IV datasets. This observation can be interpreted from a neuroscientific perspective. One possible explanation is that the 10-region brain partition aligns more accurately with the DMN, while the 7/17-region partitions are respectively too coarse or too fine to capture gender specific patterns effectively. These results demonstrate that moderate partitioning optimally balances local feature capture and global spatial modeling, whereas both coarse-graining and excessive fine-graining degrade overall model performance. Consequently, the 10-region partitioning strategy is adopted throughout all experiments.

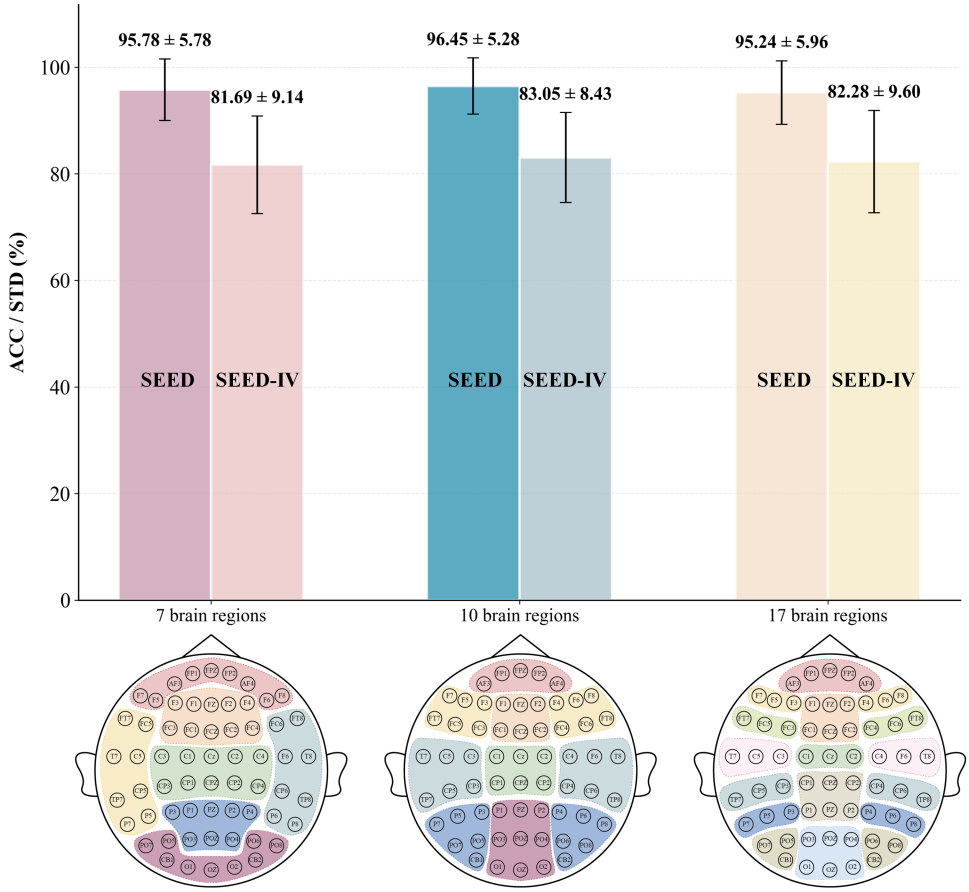

Figure 6. Comparisons of subject-dependent performance of different brain region partitioning methods on the SEED and SEED-IV datasets.

Table 1. Performance Evaluations (ACC/STD) on the SEED and SEED-IV Datasets Compared with Competing Methods.

Model	SEED		SEED-IV	
	Subject-Dependent	**Subject-Independent**	**Subject-Dependent**	**Subject-Independent**
SVM [5]	83.99/9.72	56.73/16.29	56.61/20.05	37.99/12.52
DGCNN [10]	90.40/8.49	79.95/9.02	-	-
MS-MDA [30]	-	82.67/9.51	-	67.96/11.94
Bi-HDM [8]	93.12/6.12	85.40/7.53	74.35/14.09	69.03/8.66
R2G-STNN [9]	93.38/5.96	84.16/7.63	-	-
RGNN[11]	94.24/5.95	85.30/6.72	79.27/10.54	73.84/8.02
Progressive-GCN [12]	-	-	77.08/12.43	69.44/10.16
Pyramidal-GCN [13]	**96.93/5.11**	84.59/8.68	82.24/14.85	**73.69/7.16**
OURS	96.68/4.19	**87.55/9.53**	**83.05/8.43**	73.67/4.55

- denotes that the results are not reported in the original work. The best results are marked in bold.

4.2. Gender-Specific Comparisons with Competing Methods

To investigate the existence and impact of gender differences on model performance, this subsection further conducts comparative analyses between same-gender and cross-gender training protocols by comparing the performance of different models under the two strategies. Beyond classical machine learning method SVM [5] and established graph-based approaches DGCNN [10] and RGNN [11], this experiment incorporates GSCNN [38] and ASGC [22,23] into comparative analyses. These latter two models have made considerable contributions to advancing research on the factor of gender difference in EEG-based emotion recognition.

As shown in Table 2, the models trained using the same-gender strategy (F-F and M-M) generally exhibit better performance compared to cross-gender strategy (M-F and F-M). This finding aligns closely with conclusions from previous studies [20–23] and is specially obvious on the SEED dataset. From their conclusions, this existing gender difference in EEG emotion recognition may relate to functional differentiation in brain regions at a physiological level [39]. Meanwhile, the proposed RPGCN-GDA model demonstrates significant advantages in gender-specific emotion recognition tasks, particularly excelling in generalization capabilities for cross-gender tasks. On the SEED dataset, the RPGCN-GDA achieves the accuracy of 86.47% in the M-M scenario, representing the improvements of 5.24% and 7.68% over GSCNN [38] and ASGC [22,23] in other gender-related studies, respectively. A similar trend is observed on the SEED-IV dataset, highlighting the enhanced capability of our model to discern male-specific patterns within same-gender groups. Furthermore, our method attains the accuracies of 85.01% and 82.43% in the F-M and M-F scenarios, respectively. Although these results reflect a marginal performance degradation compared to same-gender models (M-M: 86.47%; F-F: 84.55%), the decline is significantly narrower than those of other benchmark methods. In contrast, the baseline deep learning method of ASGC [22,23] performs well overall but exhibits a substantial performance gap between same-gender and cross-gender on the SEED dataset, which reflects the challenge that gender differences pose to model generalization. While our model alleviates this issue through its gender-sensitive mechanism. Notably on the SEED-IV dataset, the cross-gender models achieve comparable or even better performance than same-gender ones in some cases. It can be inferred that the gender imbalance in the SEED-IV dataset may naturally encourage the model to learn more generalized features during training. Furthermore in our method, when the GDA module effectively aligns feature distributions between genders, the proposed model can learn more comprehensive emotion representations from cross-gender samples.

4.3. Ablation Study

In this subsection, we analyze the impacts of RGE, GDA and $\mathbf{P}_{\mathcal{R}}$ to the overall performance of our model through the ablation experiments. In addition, we also explore the generalization capability of our model in cross-subject and cross-gender emotion recognition by using same-gender, cross-gender and mixed-gender strategies as shown in Tables 3 and 4. Notably, GDA defines the subject domain based on gender labels. For the same-gender strategy, both the training and testing data belong to the same domain, making no sense to cross-gender distribution adjustment. Therefore, during the training of the same-gender models, the GDA module is removed.

4.3.1. Mixed-Gender Analysis

For the mixed-gender subject-independent experiments as shown in Tables 3 and 4, compared to the backbone model (without RGE and GDA), the RGE module helps to improve the accuracy on the SEED and SEED-IV datasets by 4.33% and 3.33%, respectively. This may be attributed to the fact that the introduction of RGE enhances

the ability of model to capture gender-specific brain functional connectivity patterns and extract deeper emotional information through progressive dynamic learning. Similarly, it can be seen different degrees of improvements on both datasets after incorporating the GDA module, showcasing its domain adaptation capability. In addition, the removal of the $\mathbf{P}_{\mathcal{R}}$ also decreases overall performance under the mixed-gender protocol. This indicates that $\mathbf{P}_{\mathcal{R}}$ enhances model robustness by capturing gender-specific connectivity differences that are not addressed by global patterns alone. Ultimately, the two modules of RGE and GDA as well as $\mathbf{P}_{\mathcal{R}}$ together increase the accuracy of cross-subject emotion recognition from 77.93% to 87.55% on the SEED dataset and from 68.70% to 73.67% on the SEED-IV dataset, respectively.

Table 2. Gender-specific Performance Evaluations (ACC/STD) on the SEED and SEED-IV Datasets Compared with Competing Methods.

Dataset	Method	Same-Gender		Cross-Gender	
		M-M	F-F	F-M	M-F
SEED	SVM [5]	81.05/10.25	75.60/10.36	71.45/13.86	74.12/11.95
	DGCNN [10] *	76.19/12.67	78.55/11.45	75.23/11.34	72.45/14.43
	RGNN [11] *	82.84/8.83	79.83/9.56	79.95/10.75	77.20/13.29
	GSCNN [38] *	81.23/6.74	80.83/9.56	80.23/8.56	79.23/13.22
	ASGC [22]	78.79/5.71	**89.44/5.80**	77.18/9.50	82.17/10.50
	OURS	**86.47/5.03**	84.55/6.76	**85.01/4.37**	**82.43/6.62**
SEED-IV	SVM [5]	56.92/14.15	54.21/11.49	53.26/13.85	51.89/11.44
	DGCNN [10] *	62.12/15.96	61.79/12.46	61.23/9.77	60.65/14.61
	RGNN [11] *	67.76/10.38	68.37/10.23	68.23/10.23	65.49/12.33
	GSCNN [38] *	62.08/12.56	67.22/8.51	62.49/13.22	65.10/10.22
	ASGC [23]	71.45/7.77	70.33/4.51	70.88/8.64	70.77/9.69
	OURS	**75.14/4.50**	**70.41/10.89**	**75.24/6.35**	**73.03/5.86**

* denotes that the method is reproduced manually. The best results are marked in bold.

Table 3. Performance (ACC/STD) of Ablation Study under Different Protocols on the SEED Dataset.

Model	Same-Gender		Cross-Gender		Mixed-Gender
	M-M	F-F	F-M	M-F	
w/o RGE & GDA	80.68/5.61	78.59/8.01	75.02/7.24	76.60/9.57	77.93/7.14
w/o GDA	**86.47/5.03**	**84.55/6.76**	84.72/5.76	82.71/7.42	82.26/6.66
w/o RGE	-	-	83.93/5.58	81.67/5.38	84.91/7.27
w/o $\mathbf{P}_{\mathcal{R}}$	-	-	**87.19/7.79**	81.95/4.58	85.59/4.37
RPGCN-GDA	-	-	85.01/4.37	**82.43/6.62**	**87.55/9.53**

w/o: without the module. The best results are marked in bold.

Table 4. Performance (ACC/STD) of Ablation Study under Different Protocols on the SEED-IV Dataset.

Model	Same-Gender		Cross-Gender		Mixed-Gender
	M-M	F-F	F-M	M-F	
w/o RGE & GDA	67.33/9.49	68.55/5.56	65.14/10.37	62.62/6.25	68.70/6.45
w/o GDA	**75.14/4.50**	**70.41/10.89**	72.10/6.98	71.39/9.51	72.03/8.04
w/o RGE	-	-	74.08/5.34	71.74/7.36	70.74/6.90
w/o $\mathbf{P}_{\mathcal{R}}$	-	-	74.62/8.93	70.18/6.34	73.11/6.53
RPGCN-GDA	-	-	**75.24/6.35**	**73.03/5.86**	**73.67/4.55**

w/o: without the module. The best results are marked in bold.

4.3.2. Same-Gender and Cross-Gender Analysis

Under the gender-specific protocols, we observe from Tables 3 and 4 that the performance of the backbone models (without RGE and GDA) trained with the cross-gender strategy is generally lower than that trained with the same-gender and mixed-gender strategies. From the comparison results of M-M vs. F-M and F-F vs. M-F, the same-gender models outperform cross-gender models, which is in accord with the previous studies [20–23]. Meanwhile, the RGE and GDA modules together with $\mathbf{P}_{\mathcal{R}}$ gradually narrow the gap in performance between M-M and F-M models as well as F-F and M-F models, even expanding the performance benefits of the cross-gender models. In the terms of model optimization, despite the inherent emotional gender differences, these gender-sensitive designs in our model can mitigate these discrepancies, enabling effective cross-gender emotion recognition.

4.3.3. Gender-Imbalanced Analysis

To further evaluate the practical applicability of our model in real-world deployment where gender data is often imbalanced, we conduct additional subject-independent experiments with varying female-to-male subject ratios on the SEED dataset. Specifically, we adjust the sample sizes of female and male participants to simulate real-world imbalances. As shown in Figure 7, the proposed model achieves its highest accuracy of 87.55% when the female-to-male ratio is 8:7, which is close to gender balance. As the gender imbalance increases in either direction with more female or more male subjects, the performance gradually decreases with a predictable degradation pattern. It can be attributed to the model's inability to sufficiently learn gender-specific neural patterns when samples of one gender are scarce. Notably, when the minority gender ratio drops to nearly 30% (F:M = 8:3, F:M = 3:7), the accuracies only decrease to 83.82% and 84.73% respectively, demonstrating the model's strong robustness to imbalanced data. It is worth noting that the SEED-IV dataset itself exhibits gender imbalance (F:M = 9:6), yet our model still achieves a cross-subject accuracy of 73.67% that outperforms most existing methods. These results indicate that our model with gender-sensitive design can effectively handle the mild gender imbalances commonly found in real-world data without significant performance degradation.

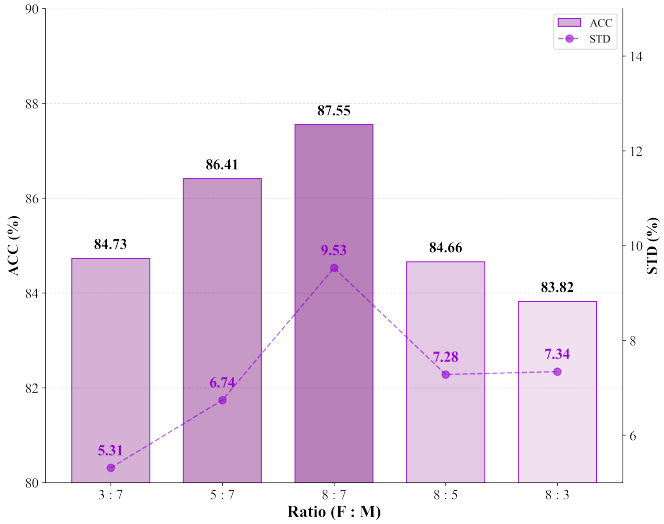

Figure 7. Subject-independent performance under gender-imbalanced scenarios. The bar chart shows the classification accuracy (ACC) while the dotted line shows the standard deviation (STD) across different female-to-male subject ratios (F:M) on the SEED dataset.

4.4. Feature Distribution Visualization via t-SNE

To investigate the progressive learning process of our model and the interaction between the GRL and graph encoders, we present t-SNE visualizations of feature distributions at four critical stages on the SEED dataset in Figure 8.

Obviously, the DE features in Figure 8a exhibit highly mixed clustering for all three emotion categories, indicating limited discriminability in raw features. However, the distribution in the gender domain shows a moderate degree of separation, suggesting that gender-specific patterns are inherently present in the raw EEG signals, even before any model processing. Then the features show initial separation for both emotion and gender after the SGE and RGE processing in Figure 8b,c. This stage effectively preserves gender-specific neural patterns that are relevant to emotional processing and the gender differences become more pronounced. Crucially, as shown in Figure 8d, the three categories of emotional features achieve maximum separation with minimal overlap and the gender distribution becomes highly mixed, demonstrating that the GDA module with GRL successfully eliminates gender distributional differences in emotional features. This process proves the GRL-based adaptation works selectively and removes gender-related features that contribute to domain shift while preserving emotion-discriminative information in mixed-gender emotion recognition tasks.

4.5. Confusion Matrix Analysis

To further analyze the gender-sensitivity of our RPGCN-GDA model and its capability to represent gender-specific emotional patterns, we visualize the prediction results as confusion matrices in Figure 9 under both same-gender and cross-gender strategies. On the SEED dataset, the model achieves high prediction accuracies

in same-gender scenarios, particularly for males in recognizing negative (M-M: 87.84%) and neutral emotions (87.07%), and for females in positive emotions (F-F: 90.11%). This indicates that the model effectively captures gender-specific neural patterns for these emotional states. The cross-gender model shows strong adaptability by achieving competitive performance in predicting positive and neutral emotions. On the SEED-IV dataset, the same-gender models show more consistent and stable emotion predictions within the female group (F-F: 81.67%, 82.28%, 70.27%, 62.81% for four categories of emotions of neutral, sad, fear, happy), while the male group exhibits more emotional variability (M-M: 59.45%, 82.75%, 76.47%, 60.45%). In cross-gender settings, our model effectively adapts to gender-specific neural variances in the category of sad (F-M: 80.57%, M-F: 86.87%). The variation in model performance across datasets and emotional states emphasizes the complexity of cross-gender emotion recognition. However, it also highlights that our model is capable of generalizing across genders by learning shared yet distinct representations of neural patterns for subtle emotions.

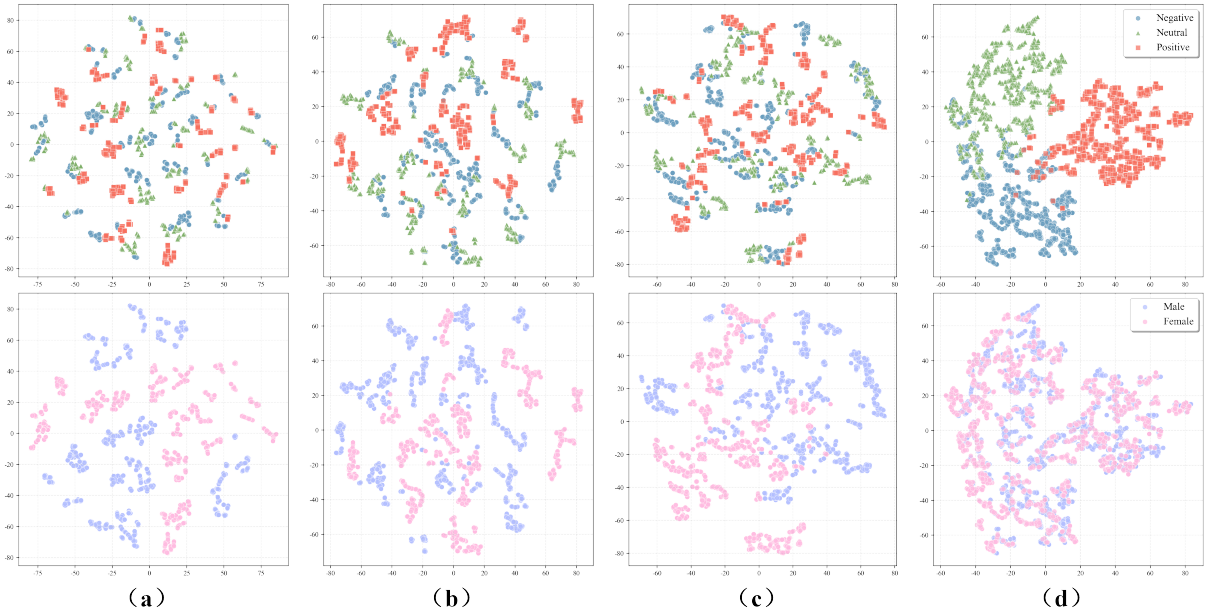

Figure 8. The visualization of the progressive feature representation learning in the RPGCN-GDA. (**a**–**d**) show the t-SNE visualizations of feature distributions at four stages of the model: (**a**) the input of DE features, (**b**) the output of SGE, (**c**) the output of RGE, and (**d**) the output of the final layer. Top row displays the clustering of emotional features on the SEED dataset, while bottom row shows gender domain clustering (male vs. female).

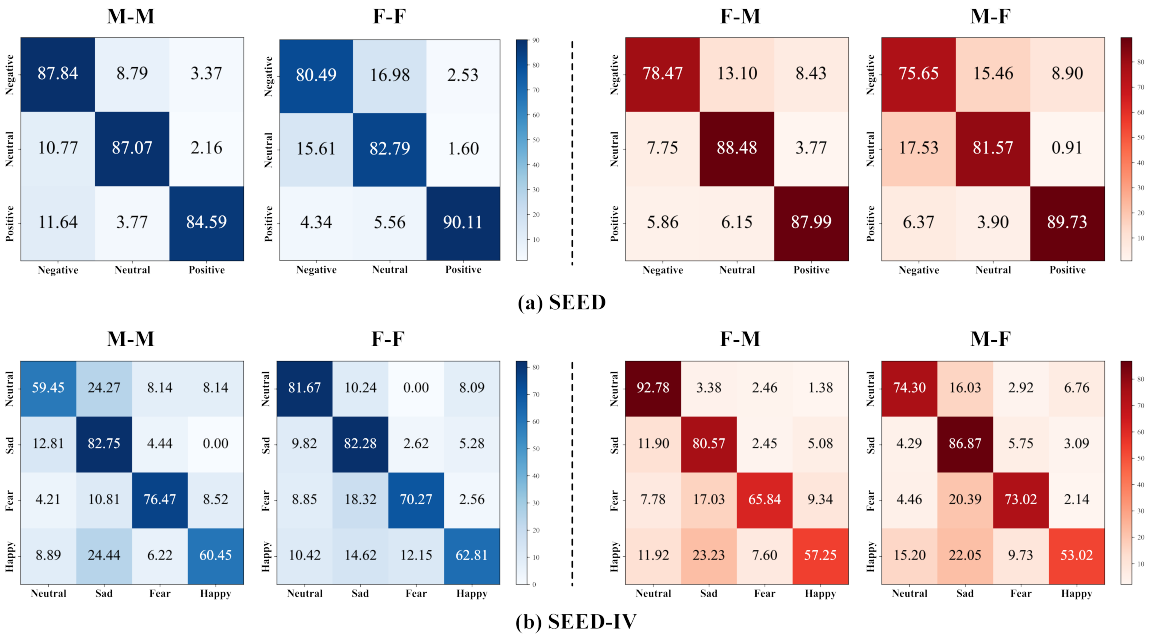

Figure 9. Confusion matrices for same-gender and cross-gender emotion recognition on the SEED and SEED-IV datasets.

4.6. Visualization Analysis of Adjacency Matrix

In the works related to GNNs, the degree centrality of an adjacency matrix is a fundamental metric to assess node importance. It evaluates the influence of one node in a graph based on the sum of connection strengths of its direct links to other nodes [40]. For an adjacency matrix $\mathbf{A}$, the degree centrality of the i-th node can be calculated as:

$$c_i = \sum_{j=1}^{n} (\mathbf{A}_{i,j}) + \sum_{k=1}^{n} (\mathbf{A}_{k,i}) - 2\mathbf{A}_{i,i}, \quad (i = 1, \ldots, n) \tag{15}$$

where n represents the total number of nodes in the graph, which corresponds to the number of EEG channels.

To investigate the mechanisms of gender sensitivity underlying individual differences in EEG-based emotion recognition, we extract the spatially adaptive adjacency matrix $\mathbf{A}_{\mathcal{S}}$ learned in a data-driven manner by the RPGCN model on the SEED dataset. As shown in Figure 10, the adjacency matrices of three male subjects (subject Nos. 5, 6, 9) and three female subjects (subject Nos. 7, 8, 10) from the SEED dataset are extracted and these subjects always achieve better results in subject-dependent experiments. We further visualize their normalized degree centrality distributions and corresponding connectivity patterns by different gender groups. Obviously, male subjects exhibit prominent high-degree centrality features primarily in the occipital and parietal lobes. In contrast, female subjects show significant high-degree centrality in the prefrontal cortex and temporal lobe. In terms of connection topology, male subjects demonstrate stronger long-range and cross-regional connections. Meanwhile, female subjects exhibit denser local connections, predominantly within the prefrontal-temporal network. These findings align closely with fMRI studies [17,41], which have revealed neural correlates of sex differences in emotional reactivity and regulation: males are more dependent on broad regional coordination and dorsal sensory integration, while females prioritize prefrontal cortical network regulation and enhanced intra-regional integration capacities. These findings further corroborate the existence of gender-specific neural patterns and provide a solid neuroscientific foundation for our model design.

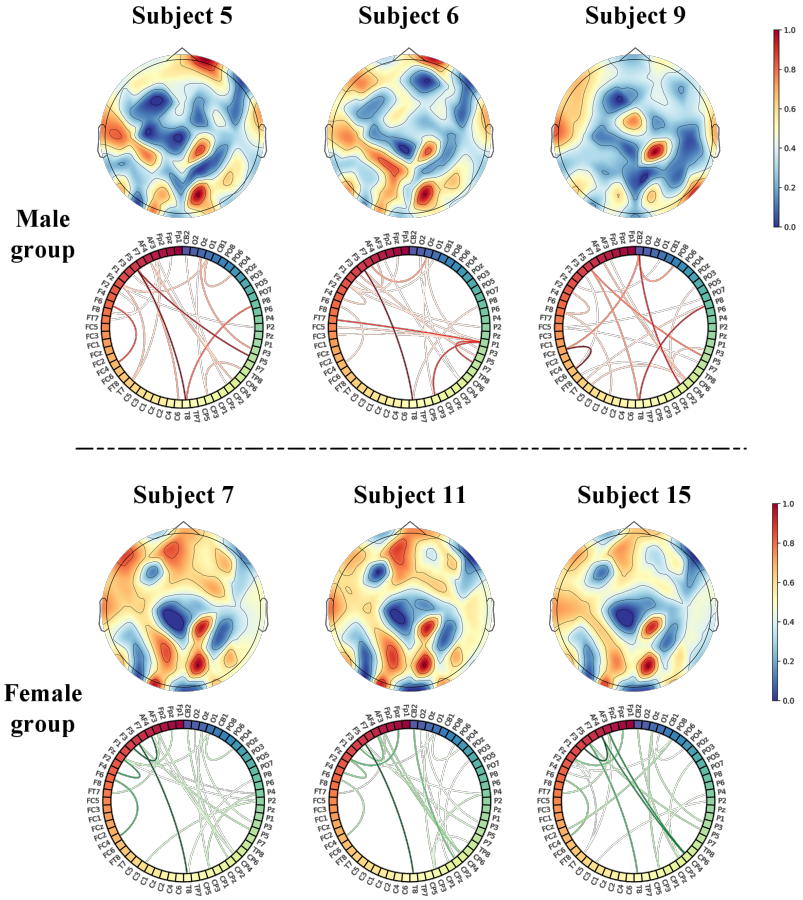

Figure 10. Visualization of degree centrality and connectivity of different gender groups on the SEED dataset. For each group, the top row displays brain topographic maps color-coded by the normalized channel-wise degree centrality, with the color scale ranging from red (highest influence) to blue (lowest influence). The bottom row shows the top 20 connections within each adjacency matrix, where the darker lines indicate stronger connections.

5. Conclusions

In this paper, we propose a regionally progressive graph convolutional network with gender-sensitive domain adaptation to address the impact of gender differences in EEG-based emotion recognition. For effectively capturing the complex dependencies between brain functional regions, a regionally progressive graph structure is designed with attention mechanism-based feature fusion. And then, we introduce a series of gender sensitive designs such as gender-specific functional connectivity weights and gender domain adaptation module, enabling our model to capture distinct neural patterns for males and females effectively. The proposed RPGCN-GDA demonstrates superior performance not only in subject-dependent and subject-independent experiments but also in gender-specific emotion recognition tasks, especially in handling cross-gender emotion recognition with strong generalization capabilities. Our model provides a scalable and interpretable solution for developing EEG-based emotion recognition systems with stronger gender sensitivity. In future work, we will systematically evaluate the cross-cultural generalizability of our gender-sensitive mechanisms by validating the model on the western datasets. This investigation will determine whether the identified gender-specific neural patterns persist across different cultural contexts, laying a solid foundation for developing robust and culturally adaptable affective computing systems.

Author Contributions

Y.H. and W.Z.: conceptualization, methodology, software; Y.H.: data curation, writing—original draft preparation; Y.H. and S.H.: visualization, investigation; S.H. and F.H.: supervision, validation; L.Y. and Q.Z.: writing—reviewing and editing; Q.Z. and S.H.: funding acquisition. All authors have read and agreed to the published version of the manuscript.

Funding

This work is supported by the National Natural Science Foundation of China under Grant Nos. 62271455 and 62501545.

Data Availability Statement

The publicly available datasets of SEED and SEED-IV can be found here: https://bcmi.sjtu.edu.cn/home/seed/index.html and we have obtained the permission to use the datasets in our research.

Conflicts of Interest

The authors declare no conflict of interest.

Use of AI and AI-assisted Technologies

No AI tools were utilized for this paper.

References

1. Li, X.; Zhang, Y.; Tiwari, P.; et al. EEG based emotion recognition: a tutorial and review. *Acm Comput. Surv.* **2022**, *55*, 1–57.
2. Zhao, S.; Hong, X.; Yang, J. Toward label-efficient emotion and sentiment analysis. *Proc. IEEE* **2023**, *111*, 1159–1197.
3. Zhao, S.; Yao, X.; Yang, J. Affective image content analysis: two decades review and new perspectives. *IEEE Trans. Pattern Anal. Mach. Intell.* **2021**, *44*, 6729–6751.
4. Wang, Y.; Zhang, B.; Di, L. Research progress of EEG-based emotion recognition: A survey. *Acm Comput. Surv.* **2024**, *56*, 1–49.
5. Wang, X.W.; Nie, D.; Lu, B.L. Emotional state classification from EEG data using machine learning approach. *Neurocomputing* **2014**, *129*, 94–106.
6. Ding, Y.; Robinson, N.; Zhang, S.; et al. TSception: capturing temporal dynamics and spatial asymmetry from EEG for emotion recognition. *IEEE Trans. Affect. Comput.* **2023**, *14*, 2238–2250.
7. Tao, W.; Li, C.; Song, R. EEG-based emotion recognition via channel-wise attention and self attention. *IEEE Trans. Affect. Comput.* **2023**, *14*, 382–393.
8. Li, Y.; Wang, L.; Zheng, W. A novel bi-hemispheric discrepancy model for EEG emotion recognition. *IEEE Trans. Cogn. Dev. Syst.* **2021**, *13*, 354–367.
9. Li, Y.; Zheng, W.; Wang, L. From regional to global brain: a novel hierarchical spatial-temporal neural network model for EEG emotion recognition. *IEEE Trans. Affect. Comput.* **2022**, *13*, 568–578.
10. Song, T.; Zheng, W.; Song, P. EEG emotion recognition using dynamical graph convolutional neural networks. *IEEE Trans. Affect. Comput.* **2020**, *11*, 532–541.

11. Zhong, P.; Wang, D.; Miao, C. EEG-based emotion recognition using regularized graph neural networks. *IEEE Trans. Affect. Comput.* **2022**, *13*, 1290–1301.
12. Zhou, Y.; Li, F.; Li, Y.; et al. Progressive graph convolution network for EEG emotion recognition. *Neurocomputing* **2023**, *544*, 126262–126273.
13. Jin, M.; Du, C.; He, H. PGCN: pyramidal graph convolutional network for EEG emotion recognition. *IEEE Trans. Multimed.* **2024**, *26*, 9070–9082.
14. Power, J.D.; Cohen, A.L.; Nelson, S.M. Functional network organization of the human brain. *Neuron* **2011**, *72*, 665–678.
15. Nolen-Hoeksema, S. Gender differences in depression. *Curr. Dir. Psychol. Sci.* **2001**, *10*, 173–176.
16. Thayer, J.F.; Rossy, L.A.; Ruiz-Padial, E. Gender differences in the relationship between emotional regulation and depressive symptoms. *Cogn. Ther. Res.* **2003**, *27*, 349–364.
17. Stevens, J.S.; Hamann, S. Sex differences in brain activation to emotional stimuli: a meta-analysis of neuroimaging studies. *Neuropsychologia* **2012**, *50*, 1578–1593.
18. Weiss, E.; Siedentopf, C.M.; Hofer, A. Sex differences in brain activation pattern during a visuospatial cognitive task: a functional magnetic resonance imaging study in healthy volunteers. *Neurosci. Lett.* **2003**, *344*, 169–172.
19. Zhu, J.Y.; Zheng, W.L.; Lu, B.L. Cross-subject and cross-gender emotion classification from EEG. In Proceedings of the World Congress on Medical Physics and Biomedical Engineering, Toronto, Canada, 7–12 June 2015.
20. Yan, X.; Zheng, W.L.; Liu, W. Investigating gender differences of brain areas in emotion recognition using LSTM neural network. In Proceedings of the 24th International Conference on Neural Information Processing, Guangzhou, China, 14–18 November 2017.
21. Yan, X.; Zheng, W.L.; Liu, W. Identifying gender differences in multimodal emotion recognition using bimodal deep autoencoder. In Proceedings of the 24th International Conference on Neural Information Processing, Guangzhou, China, 14–18 November 2017.
22. Li, Z.; Liu, L.; Zhu, Y. Exploring sex differences in key frequency bands and channel connections for EEG-based emotion recognition. In Proceedings of the 44th Annual International Conference of the IEEE Engineering in Medicine & Biology Society, Glasgow, UK, 11–15 July 2022.
23. Peng, D.; Zheng, W.L.; Liu, L. Identifying sex differences in EEG-based emotion recognition using graph convolutional network with attention mechanism. *J. Neural Eng.* **2023**, *20*, 066010–066029.
24. Wu, F.; Souza, A.; Zhang, T. Simplifying graph convolutional networks. In Proceedings of the 36th International Conference on Machine Learning, Long Beach, CA, USA, 9–15 June 2019.
25. Duan, R.N.; Zhu, J.Y.; Lu, B.L. Differential entropy feature for EEG-based emotion classification. In Proceedings of the 6th International IEEE/EMBS Conference on Neural Engineering, San Diego, CA, USA, 6–8 November 2013.
26. Alarcao, S.M.; Fonseca, M.J. Emotions recognition using EEG signals: A survey. *IEEE Trans. Affect. Comput.* **2019**, *10*, 374–393.
27. Jin, W.; Derr, T.; Wang, Y. Node similarity preserving graph convolutional networks. In Proceedings of the 14th ACM International Conference on Web Search and Data Mining, Virtual, 8–12 March 2021.
28. Gu, R.F.; Li, R.; Lu, B.L. Cross-subject decision confidence estimation from EEG signals using spectral-spatial-temporal adaptive GCN with domain adaptation. In Proceedings of International Joint Conference on Neural Networks, Gold Coast, Australia, 18–23 June 2023.
29. Ju, X.; Wu, X.; Dai, S. Domain adversarial learning with multiple adversarial tasks for EEG emotion recognition. *Expert Syst. Appl.* **2025**, *266*, 126028–126048.
30. Chen, M.; Jin, M.; Li, Z. MS-MDA: multisource marginal distribution adaptation for cross-subject and cross-session EEG emotion recognition. *Front. Neurosci.* **2021**, *15*, 778488–778498.
31. Ganin, Y.; Ustinova, E.; Ajakan, H.; et al. Domain-adversarial training of neural networks. *J. Mach. Learn. Res.* **2016**, *17*, 1–35.
32. Tzeng, E.; Hoffman, J.; Saenko, K.; et al. Adversarial discriminative domain adaptation. In Proceedings of the IEEE Conference on Computer Vision and Pattern Recognition, Honolulu, HI, USA, 21–26 July 2017.
33. Li, C.; Zhang, Y.; Zheng, L.; et al.. An efficient graph learning system for emotion recognition inspired by the cognitive prior graph of EEG brain network. *IEEE Trans. Neural Netw. Learn. Syst.* **2025**, *36*, 7130–7144.
34. Zheng, W.L.; Lu, B.L. Investigating critical frequency bands and channels for EEG-based emotion recognition with deep neural networks. *IEEE Trans. Auton. Ment. Dev.* **2015**, *7*, 162–175.
35. Zheng, W.L.; Liu, W.; Lu, Y.; et al. EmotionMeter: a multimodal framework for recognizing human emotions. *IEEE Trans. Cybern.* **2019**, *49*, 1110–1122.
36. Ye, M.; Chen, C.L.P.; Zhang, T. Hierarchical dynamic graph convolutional network with interpretability for EEG-based emotion recognition. *IEEE Trans. Neural Netw. Learn. Syst.* **2022**. https://doi.org/10.1109/TNNLS.2022.3225855.
37. Gong, G.; He, Y.; Evans, A.C. Brain connectivity: gender makes a difference. *Neuroscientist* **2011**, *17*, 575–591.
38. Duan, D.; Li, Q.; Zhong, W. GSCNN: gender-sensitive EEG emotion recognition using convolutional neural network. In Proceedings of the International Conference on Mechatronics and Machine Vision in Practice, Queenstown, New Zealand, 21–24 November 2023.
39. Proverbio, A.M. Sex differences in the social brain and in social cognition. *J. Neurosci. Res.* **2023**, *101*, 730–738.

40. Zhang, X.; Cheng, G.; Qu, Y. Ontology summarization based on rdf sentence graph. In Proceedings of the 16th International Conference on World Wide Web, Banff, AB, Canada, 8–12 May 2007.
41. Domes, G.; Schulze, L.; Böttger, M. The neural correlates of sex differences in emotional reactivity and emotion regulation. *Hum. Brain Mapp.* **2010**, *31*, 758–769.